PHYSICAL REVIEW D **93,** 101902(R) (2016)

Self-similar equilibration of strongly interacting systems from holography

Ioannis Bakas,[1] Kostas Skenderis,[2] and Benjamin Withers[2,3,4]

[1]*Department of Physics, School of Applied Mathematics and Physical Sciences, National Technical University, 15780 Athens, Greece*

[2]*STAG Research Centre and Mathematical Sciences, University of Southampton, Southampton SO17 1BJ, United Kingdom*

[3]*School of Mathematical Sciences, Queen Mary University of London, Mile End Road, London E1 4NS, United Kingdom*

[4]*DAMTP, Centre for Mathematical Sciences, Wilberforce Road, Cambridge CB3 0WA, United Kingdom*

(Received 9 February 2016; published 23 May 2016)

We study the equilibration of a class of far-from-equilibrium strongly interacting systems using gauge-gravity duality. The systems we analyze are $2+1$ dimensional and have a four-dimensional gravitational dual. A prototype example of a system we analyze is the equilibration of a two-dimensional fluid which is translational invariant in one direction and is attached to two different heat baths with different temperatures at infinity in the other direction. We realize such setup in gauge-gravity duality by joining two semi-infinite asymptotically anti-de Sitter (AdS) black branes of different temperatures, which subsequently evolve towards equilibrium by emitting gravitational radiation towards the boundary of AdS. At sufficiently late times the solution converges to a similarity solution, which is only sensitive to the left and right equilibrium states and not to the details of the initial conditions. This attractor solution not only incorporates the growing region of equilibrated plasma but also the outwardly propagating transition regions, and can be constructed by solving a single ordinary differential equation.

DOI: 10.1103/PhysRevD.93.101902

I. INTRODUCTION

Far-from-equilibrium dynamics is a topic of considerable interest, yet it is theoretically poorly understood, particularly for strongly interacting systems which do not admit a quasiparticle picture. In this paper we aim to use gauge-gravity duality to study the equilibration process for a class of strongly interacting systems. Through the duality, thermal states are dual to stationary AdS black holes. Away from equilibrium, the system is described by the evolution of the Einstein equations subject to appropriate boundary conditions at the AdS boundary.

There has been a strong interest in the application of holographic techniques to out-of-equilibrium phenomena, including examples in thermalization [1], heavy ion collisions [2,3], turbulence [4], and dynamical and stationary quenches in normal and superfluid phases [5,6], to name a few. Typically, numerical techniques are required to evolve the Einstein equations, but with certain simplifying assumptions, simpler models can be used to shed some light on the underlying physics, for example, the use of the analytic Vaidya spacetime in the context of thermalization [7].

In this paper we study the evolution of $2+1$-dimensional systems (thin films) which are translational invariant in one direction and are attached to conformally invariant heat baths with different temperatures in the other direction. There has been a recent interest in the study of such configurations, with a universal steady-state flow conjectured to emerge in the equilibrating region [8–12]. Explicit constructions of gravitational dual solutions show agreement [13] with the proposed ansatz.

We show that this setup can be captured by the Robinson-Trautman (RT) class of solutions to the Einstein equations [14]. The RT spacetimes are 4d solutions which can be constructed by solving a single 3d parabolic partial differential equation (PDE) for a field σ, which includes the asymptotically AdS spacetimes of interest here. Remarkably, the equation that one gets is qualitatively similar to the one that appeared in earlier studies of thin films (see [15] for a review).

By choosing appropriate boundary conditions for σ, we can set up the situation described above, wherein we join two different thermal states and study the evolution towards equilibrium. Remarkably, we find that at sufficiently late times the process of equilibration is only sensitive to the left and right thermal states, and becomes independent of any other details of the initial conditions. The universal solution is similarity invariant and is governed by an ordinary differential equation (ODE). The use of RT solutions in the context of AdS/CFT has been studied in [16,17].

One important aspect of the RT solutions is that the boundary metric is inhomogeneous and time dependent, in concert with the state of the quantum system. This can be viewed as resulting from deformations of the CFT which ensure that the bulk metric is of RT type. In other words, the Hamiltonian of the system is time dependent and becomes conformally invariant at late times. As such, our results are not expected to agree directly with those of [8–13]. Nevertheless, we have described a new class of universal late-time gravitational behavior governing far-from-equilibrium CFTs with deformations; it would be interesting to see whether such self-similar phenomena have wider applicability, for instance, beyond the scope of the RT solutions themselves and to other CFT settings where the deformations may be better understood.

II. ROBINSON-TRAUTMAN

The RT solutions can be viewed as a nonlinear generalization of algebraically special perturbations of 4d Schwarzschild black holes which describe purely outgoing gravitational radiation. These perturbations can be lifted to a nonlinear solution, resulting in a time-dependent, inhomogeneous spacetime possessing a shear-free, irrotational null geodesic congruence. RT solutions exist for any value of the cosmological constant Λ. Here we take the case of asymptotically locally AdS spacetimes, with $\Lambda = -3/L^2$. In retarded time u, the line element is given by

$$ds^2 = -F du^2 - 2du dr + \frac{r^2}{\sigma^2}(dx^2 + dy^2), \tag{1}$$

$$F \equiv -\frac{\Lambda}{3} r^2 - 2r \frac{\partial_u \sigma}{\sigma} + \sigma^2 \nabla^2_{R^2} \log \sigma - \frac{2m}{r}, \tag{2}$$

where $\nabla^2_{R^2}$ is the standard Laplacian for R^2. This line element satisfies Einstein equations provided $\sigma(u,x,y)$ satisfies a certain fourth-order nonlinear parabolic equation on R^2. This equation can be phrased as a geometric flow; let us define a Euclidean 2-metric

$$\gamma_{ij}(u,x,y) dx^i dx^j = \frac{1}{\sigma^2(u,x,y)}(dx^2 + dy^2). \tag{3}$$

Then γ obeys the Calabi flow equation, i.e.,

$$\partial_u \gamma_{ij} = \frac{1}{12m} \nabla^2_\gamma R_\gamma \gamma_{ij} \tag{4}$$

which is now an equation for σ, where ∇^2_γ and R_γ are the Laplacian and Ricci scalar for γ. Note that this equation is insensitive to Λ. Also note that because of the application we have in mind, we have restricted ourselves to Calabi flow on R^2.

With $\Lambda < 0$ the bulk evolution corresponding to a solution of (4) is holographically dual to an out-of-equilibrium CFT on a time-dependent, inhomogeneous background metric g, given by

$$g_{\mu\nu} dx^\mu dx^\nu = -dt^2 + \gamma_{ij}(t,x,y) dx^i dx^j, \tag{5}$$

where we have introduced the time coordinate t which is given by the value of u at the conformal boundary. For constant σ the bulk geometry is the Schwarzschild black brane solution, and the CFT is in thermal equilibrium on Minkowski space.

In this work we have taken the spatial part of the metric (5) to be noncompact. For compact cases, given smooth initial data for σ, the solution converges to a constant at late times with corrections which vanish exponentially fast with u [18–22]. Thus, in the compact case, the system settles down to the equilibrium Schwarzschild solution. This result does not apply to our planar solutions. In fact, we will see that depending on boundary conditions at spatial infinity, the system converges to a time-evolving similarity solution with polynomial corrections at late times.

III. SIMILARITY

The Calabi flow equation (4) is a fourth-order parabolic PDE, which, as we show, admits similarity solutions that play an important role in the nonlinear dynamics of the CFT. First, as a warm-up example of similarity in such systems, consider instead the heat equation, $\frac{\partial f}{\partial t} = D \frac{\partial^2 f}{\partial x^2}$, where D is the thermal diffusivity. This admits solutions with the scaling symmetry, $x \to \lambda^2 x$, $t \to \lambda t$, which are easily obtained by writing f as a function of a single invariant variable, $f(t,x) = h(\mu(x,t))$, where $\mu(t,x) = x/\sqrt{t}$. In doing so, the equation is reduced to an ODE, and one solution is

$$h = a + b\,\mathrm{erf}\left(\frac{\mu}{2\sqrt{D}}\right) \tag{6}$$

where erf is the error function and a, b are integration constants. Here, h becomes a constant as $x \to \pm\infty$ for fixed t. This solution corresponds to the evolution resulting from initially joining two semi-infinite systems of different temperatures; at $t = 0$ the solution is a step function centered on $x = 0$ where the two infinite systems are initially joined.

We can analogously look for similarity solutions of the Calabi flow equation, which, if they exist for similar boundary conditions, describe the evolution resulting from a particular way of connecting two equilibrium black brane solutions. The two different black branes should have different temperatures (and hence different masses), and this corresponds to having σ approach different values at infinity.

As a first step we note that the RT metric (1) is invariant if we make the following scalings,

$$\begin{aligned} &u \to \lambda_u u, \qquad x \to \lambda_x x, \qquad y \to \lambda_x y, \\ &r \to \lambda_u^{-1} r, \qquad m \to \lambda_u^{-3} m, \qquad \sigma \to \lambda_x \lambda_u^{-1} \sigma. \end{aligned} \tag{7}$$

For $m = 0$ this corresponds generically to a Lifshitz scaling isometry. As expected however, at finite temperature the symmetry is broken by m, which itself must scale appropriately. We do not consider the $m = 0$ limit here, and so we will always be in the broken setting; the algebraically special modes are nonanalytic at $m = 0$, and we return to this limit in [23].

We now impose translational invariance in the y direction (so, in particular, σ is independent of y), and as with the heat equation example we seek solutions which are manifestly scale invariant. As we shall see momentarily, an ansatz appropriate for (7) is

$$\sigma(t,x) = m^{1/4}(t-t_0)^p h(\mu(t,x)), \tag{8}$$

where $\mu(t,x) \equiv (x-x_0)/(t-t_0)^{p+\frac{1}{4}}$ and t_0 and x_0 are parameters corresponding to time translations and spatial translations, respectively, and they correspond to the location of the "join." We have allowed for an additional parameter p, extending the family of similarity solutions. For this ansatz (4) becomes an m-independent ODE,

$$\partial_\mu^4 h = \frac{(\partial_\mu^2 h)^2}{h} + 3(1+4p)\mu\frac{\partial_\mu h}{h^4} - \frac{12p}{h^3}. \tag{9}$$

Note that this equation has a scaling symmetry,

$$h \to \lambda h, \qquad \mu \to \lambda\mu. \tag{10}$$

Compatibility with the bulk scaling property (7) requires $\lambda = \lambda_x/\lambda_u^{p+1/4}$. As we shall see below, explicit solutions h of (9) do not transform as $\mu \to \lambda\mu$, and thus λ must be equal to one [so that (10) holds identically]. This then fixes the Lifshitz dynamical critical exponent to be $z = (p+1/4)^{-1}$. For concreteness we now focus on the case $z=4$, $p=0$—we find similar behavior for $p \neq 0$ solutions, which we turn to at the end.

To solve (9) we begin by looking for solutions describing the equilibration of nearby thermal states; i.e., we linearize about the particular $p=0$ solution $h=1$, $h(\mu) = 1+\epsilon j(\mu)$, where we have introduced a small parameter ϵ. Here, j satisfies

$$\partial_\mu^4 j = 3\mu\partial_\mu j \tag{11}$$

which admits a solution in terms of hypergeometric functions. The solution which is regular for all μ and asymptotes to a constant is given by

$$j = \frac{-3^{\frac{1}{4}}4\mu}{\Gamma(-\frac{1}{4})}\,{}_1F_3\left(\begin{matrix}\frac{1}{4}\\ \frac{1}{2},\frac{3}{4},\frac{5}{4}\end{matrix};\frac{3\mu^4}{64}\right) - \frac{\Gamma(\frac{3}{4})\mu^3}{\sqrt{2}3^{\frac{1}{4}}\pi}\,{}_1F_3\left(\begin{matrix}\frac{3}{4}\\ \frac{5}{4},\frac{3}{2},\frac{7}{4}\end{matrix};\frac{3\mu^4}{64}\right). \tag{12}$$

Here, $\lim_{\mu\to-\infty} j = -1$, $\lim_{\mu\to\infty} j = 1$ and $j(0) = 0$. This is the general solution at this order in perturbations; other constant boundary conditions can be reached using linearity and shift symmetry. We plot j in the top panel of Fig. 2.

To go to widely separated left and right thermal states, we proceed numerically. In detail, we use sixth-order finite differences in a compactified spatial coordinate, $R = \tanh(\frac{\mu}{\ell})$, where ℓ is chosen so that a uniform grid in R usefully covers the region in μ where h is varying significantly. For the examples below we have taken $\ell = 20$. The system is solved using a Newton-Raphson method, giving Dirichlet boundary conditions at $R = \pm 1$ corresponding to the constant asymptotic values of h. For concreteness we fix

$$h(R=-1) = 1, \qquad h(R=1) = 1+C. \tag{13}$$

Any other pair can be brought into this form using the symmetry (10). Some solutions are shown in Fig. 1, with a clear deviation from the linearized solution for sufficiently large C.

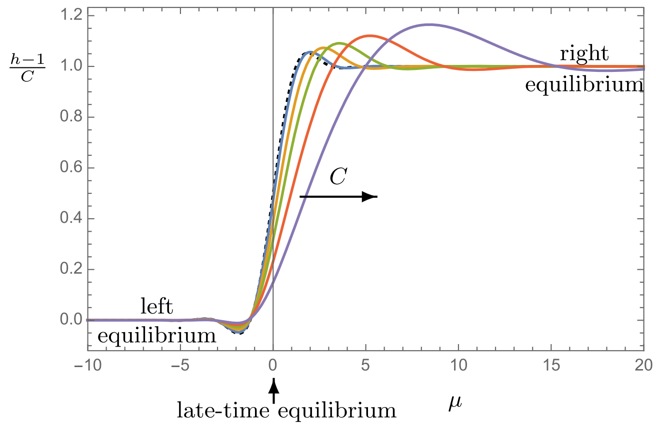

FIG. 1. Cohomogeneity-1 similarity solutions to the Calabi-flow equation on the plane. The coordinate μ, defined in (8), is a scale-invariant quantity, so the spatial profile is expanding with time. The solid curves show different values of C which label the equilibrium state of the right-hand asymptotic system as a Dirichlet boundary condition (13). The values from left to right are $C = 0.1, 0.5, 1.0, 2.0, 4.0$ and the dashed curve is the linear solution (12).

IV. QFT INTERPRETATION

In order to interpret the similarity solutions in the face of the inhomogeneous evolving boundary metric (5), on the boundary we can simultaneously perform a Weyl transformation and coordinate transformation. It is possible to do so such that for $|x| \gg t^{1/4}$ and $|x| \ll t^{1/4}$, the metric is simply $ds^2 = -dt^2 + L^2(dx^2+dy^2)$. In this frame we can simultaneously discuss the equilibrium state of the system on the left and the right and observe a growing flat space region in the interior as part of an out-of-equilibrium evolution. This can be achieved through the Weyl transformation $g_{\mathrm{new}} = \Omega^{8/3} g$ together with the coordinate transformations

$$x^i \to x^{i'} = \frac{x^i}{\Omega^{1/3}}, \qquad t \to t' = \frac{t}{\Omega^{4/3}}, \tag{14}$$

for

$$\Omega(\mu) = \sigma - \frac{\mu}{1!}\sigma' + \frac{\mu^2}{2!}\sigma'' - \frac{\mu^3}{3!}\sigma''' + \frac{\mu^4}{4!}\sigma'''', \tag{15}$$

where primes denote derivatives with respect to μ.

One may extract the holographic stress tensor from the asymptotics of the solution near the conformal infinity [24]. For RT solutions this has been done in [16,17]. The stress energy tensor may be expressed as a sum of a stress energy tensor due to a conformal perfect fluid and a part that depends on the Cotton tensor of the boundary metric [16,25]. In the left and right asymptotic regions the holographic stress tensor is simply

$$\kappa^2 \langle T^{\pm}_{\mu\nu} \rangle = \frac{m}{\sigma_{\pm}^4}\,\mathrm{diag}\left(\frac{2}{L^2}, 1, 1\right) \tag{16}$$

where the $\pm$ labels values at $x \to \pm\infty$. In the growing central region $|x| \ll t^{1/4}$ the stress tensor is

$$\kappa^2 \langle T^{0}_{\mu\nu} \rangle = \frac{m}{\sigma(0)^4}\,\mathrm{diag}\left(\frac{2}{L^2}, 1, 1\right) + \Pi_{\mu\nu} \tag{17}$$

where the additional term,

$$\Pi_{\mu\nu} dx^\mu dx^\nu = -\frac{L^2}{4}\frac{1}{t^{3/2}}\frac{\sigma''(0)}{\sigma(0)}(dx^2 - dy^2) + \frac{1}{t^{3/4}}\left(\frac{\sigma'''(0)}{\sigma(0)} - \frac{\sigma'(0)\sigma''(0)}{\sigma(0)^2}\right) dt dx, \tag{18}$$

represents the energy flow across this region and it originates from the Cotton tensor. This contribution dilutes with time, resulting in a third equilibrium region for $|x| \ll t^{1/4}$ at sufficiently large t. Corrections to these expressions appear with size $O(xt^{-1/4})$.

We can illustrate these three regions by turning to the energy density of the linear solution describing nearby equilibria, Eq. (12). The energy density can be defined by solving the following eigenvalue problem,

$$T^\mu{}_\nu u^\nu = -\varepsilon u^\mu, \tag{19}$$

where u^μ is a timelike unit-normed vector. For the frame defined in (15),

$$\varepsilon = \frac{2m}{L^2\kappa^2}\left(1 - 4\epsilon\left(j - \mu j' + \frac{1}{2!}\mu^2 j'' - \frac{1}{3!}\mu^3 j''' + \frac{1}{4!}\mu^4 j''''\right)\right). \tag{20}$$

With u^μ known, we can define two spacelike, unit-normed orthogonal vectors n_1 and n_2 which are also orthogonal to u. These are chosen such that in equilibrium n_1 is the unit vector in the x direction. Using these we can define pressures,

$$P_1 = T_{\mu\nu} n_1^\mu n_1^\nu, \qquad P_2 = T_{\mu\nu} n_2^\mu n_2^\nu. \tag{21}$$

For the linear solutions in the frame (15),

$$P_{1,2} = \frac{\varepsilon}{2} \mp \epsilon \frac{\mu j''' + 2j''}{8\kappa^2 t^{3/2}}, \tag{22}$$

where ε is given in (20). The off-diagonal term $T_{\mu\nu} n_1^\mu n_2^\nu = O(\epsilon)^2$. The energy density and pressure are shown in the lower two panels of Fig. 2, where we plot $\widehat{\delta\varepsilon} \equiv \partial_\epsilon \varepsilon|_{\epsilon=0}/(\varepsilon|_{\epsilon=0})$, and $\widehat{\delta P} \equiv \epsilon^{-1}\kappa^2 t^{3/2}(P_2 - P_1)$ as a function of μ. We can see the emergence of the equilibrium state situated between the two reservoirs, whose spatial extent grows like $t^{1/4}$. This is the thermal state reached at sufficiently late times for any fixed x.

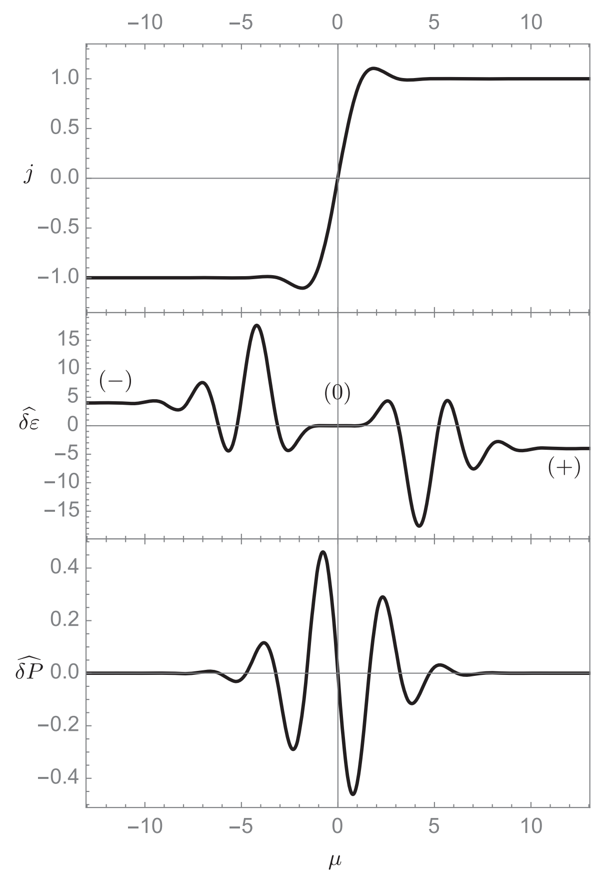

FIG. 2. The similarity solution describing closely separated equilibria, after performing a certain Weyl transformation. Top panel: The function j describing the deviation from equilibrium for the metric function σ. Middle panel: The energy density obtained from the eigenvalue equation, $\widehat{\delta\varepsilon}$, which shows the deviation from equilibrium and is defined in the text. The energy density is independent of time at fixed $x/t^{1/4}$ for each of the three flat space regions labeled by (−), (0), (+). The central equilibrium region has a spatial extent which grows as $t^{1/4}$. Bottom panel: The time-rescaled difference between longitudinal and transverse pressures, $\widehat{\delta P}$, also defined in the text.

V. STABILITY

The similarity solutions that have been discussed hitherto are not only simple examples of possible evolutions, but they also play a crucial role in determining the late-time behavior of the system. For the evolution of initial data which falls outside of the ansatz (8), the system is not initially described by a similarity solution but does settle down to the similarity solution at sufficiently late times, as prescribed by the left and right asymptotic equilibria. As a first step to establishing this result, we consider a perturbation, χ, to the similarity solution within the RT class which preserves the left and right asymptotics,

$$\sigma(t,x) = m^{\frac{1}{4}}\left(h\left(\frac{x}{t^{1/4}}\right) + \chi\left(\frac{x}{t^{1/4}}, t\right)\right). \tag{23}$$

The resulting linear PDE for χ admits separable solutions with power law decay,

$$\chi = t^{-\Delta}\chi_\Delta\left(\frac{x}{t^{1/4}}\right), \tag{24}$$

where χ_Δ satisfies the following eigenvalue problem,

$$\mathcal{O}\chi_\Delta = \Delta\chi_\Delta,$$
$$\mathcal{O} \equiv \frac{1}{12}h^4\partial_\mu^4 - \frac{1}{6}h^3h''\partial_\mu^2 - \frac{1}{4}\mu\partial_\mu + \frac{1}{12}h^2(h'')^2 + \mu\frac{h'}{h}. \tag{25}$$

The scaling (23) suggests that the dynamics of the system is governed by a Lifshitz invariant critical point with dynamical exponent $z = 4$, with the set of χs associated with the spectrum of operators of this (nonrelativistic) scale invariant theory.

The operator $\mathcal{O}$ admits a zero mode, $\chi_0 = h - \mu h'$, which follows from the invariance noted earlier (10). However, this does not preserve the boundary conditions and so can be excluded from the late-time spectrum. The spectrum about an $h = 1$ background solution can be built in reference to the perturbative solutions j, Eq. (12). The equation that χ_Δ satisfies does not depend on j at order ϵ^0,

$$\frac{1}{12}\partial_\mu^4\chi_\Delta - \frac{1}{4}\mu\partial_\mu\chi_\Delta = \Delta\chi_\Delta + O(\epsilon). \tag{26}$$

Nevertheless, a set of solutions to (26) which respect the boundary conditions are generated by solutions j, i.e.,

$$\chi_{n/4} = \partial_\mu^n j + O(\epsilon), \qquad n \in \mathbb{Z}^+. \tag{27}$$

The $n = 0$ case has been excluded because it changes the asymptotics of σ (as noted above). At least around the $h = 1$ background, we therefore have a spectrum of modes which is decaying, since $\Delta > 0$. We may reasonably expect a positive spectrum to persist in the neighborhood of the $h = 1$ backgrounds. We have verified this by numerically computing the eigenvalue spectrum of $\mathcal{O}$ for the nonlinear case, identifying the four longest lived modes as $\Delta = 1/4, 1/2, 3/4, 1$, invariant over a wide range of nonlinear similarity solutions, h. Actually, for nonlinear backgrounds we can construct two of these eigenfunctions exactly, $\chi_{1/4} = h'$ and $\chi_1 = \mu h'$. These correspond to modes which translate the solution in x and t, respectively.

VI. NUMERICAL EVIDENCE

We now turn to a general numerical evolution of the Calabi flow equation (4) in the cohomogeneity-1 case, choosing initial conditions which are incompatible with the ansatz (8). For time evolution we use Crank-Nicolson, and for each implicit stage of the integration we use Newton-Raphson for sixth-order finite differences with the same discretization of the compactified coordinate R as before.

By way of a concrete representative example in Fig. 3, we show the evolution of h for the initial data,

$$\sigma(0,x) = 1 + \frac{2}{10}\tanh x + \frac{1}{1+x^2}. \tag{28}$$

At late times the solutions approach the similarity solutions labeled by the left and right temperatures.

VII. AWAY FROM $p = 0$

We have studied in detail the cases corresponding to $p = 0$, for the primary reason that it includes the case of a thermal state on Minkowski space. For $p \neq 0$, constant σ is no longer a solution, and indeed σ can become singular, but in principle, these cases should not be excluded. For example, the following solution,

$$h = \sqrt{2}(1+\sqrt{2}\mu)^{\frac{3}{4}}, \qquad m = 1/4 \quad p = 3/4, \tag{29}$$

is the planar analogue of a solution on S^2 which contains an AdS C-metric in the bulk (see [26]). It would be interesting to investigate different values of p in more detail.

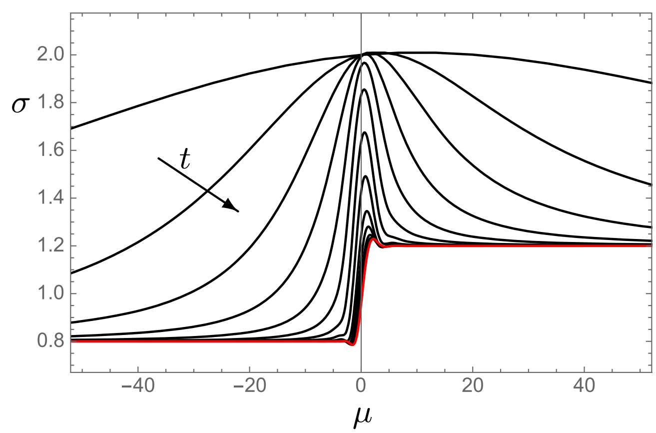

FIG. 3. Evolution of the initial data (28) according to Eq. (4), showing convergence to the planar similarity solution in red, which is prescribed only by $\sigma_\pm$. Each curve shows a different time in the evolution.

Additionally, we note that there are similarity solutions which are rotationally invariant corresponding to a different physical setup—we will describe this and related cases in more detail in a forthcoming work [23].

VIII. CONCLUSIONS

We presented a holographic study of equilibration of a class of strongly interacting systems. In particular, we holographically engineered $2+1$-dimensional systems which at $t=0$ are described by two different thermal states infinitely separated in one direction, and then studied the subsequent evolution. It turns out that the final state is a self-similar solution which only depends on the left and right temperatures and not on the details of the initial conditions. The self-similar solutions are Lifshitz invariant, and perturbations around them are governed by the spectrum of operators of an underlying Lifshitz critical theory. Our discussion should thus be applicable to all systems which are in the same universality class with this critical point.

ACKNOWLEDGMENTS

The research of I.B. is partially supported and implemented under the ARISTEIA action of the operational programme for education and lifelong learning and is co-funded by the European Social Fund (ESF) and National Resources of Greece. K.S. is supported in part by the Science and Technology Facilities Council (Consolidated Grant "Exploring the Limits of the Standard Model and Beyond"). B.W. is supported by European Research Council Grant No. ERC-2014-StG639022-NewNGR.

[1] V. Balasubramanian, A. Bernamonti, J. de Boer, N. Copland, B. Craps, E. Keski-Vakkuri, B. Muller, A. Schafer, M. Shigemori, and W. Staessens, Holographic thermalization, Phys. Rev. D **84**, 026010 (2011).

[2] R. A. Janik, The dynamics of quark-gluon plasma and AdS/CFT, Lect. Notes Phys. **828**, 147 (2011).

[3] P. M. Chesler and L. G. Yaffe, Holography and off-center collisions of localized shock waves, J. High Energy Phys. 10 (2015) 070.

[4] A. Adams, P. M. Chesler, and H. Liu, Holographic Turbulence, Phys. Rev. Lett. **112**, 151602 (2014).

[5] M. J. Bhaseen, J. P. Gauntlett, B. D. Simons, J. Sonner, and T. Wiseman, Holographic Superfluids and the Dynamics of Symmetry Breaking, Phys. Rev. Lett. **110**, 015301 (2013).

[6] P. Figueras and T. Wiseman, Stationary Holographic Plasma Quenches and Numerical Methods for Non-Killing Horizons, Phys. Rev. Lett. **110**, 171602 (2013).

[7] S. Bhattacharyya and S. Minwalla, Weak field black hole formation in asymptotically AdS spacetimes, J. High Energy Phys. 09 (2009) 034.

[8] D. Bernard and B. Doyon, Energy flow in non-equilibrium conformal field theory, J. Phys. A **45**, 362001 (2012).

[9] D. Bernard and B. Doyon, Time-reversal symmetry and fluctuation relations in non-equilibrium quantum steady states, J. Phys. A **46**, 372001 (2013).

[10] H.-C. Chang, A. Karch, and A. Yarom, An ansatz for one dimensional steady state configurations, J. Stat. Mech. (2014) P06018.

[11] M. J. Bhaseen, B. Doyon, A. Lucas, and K. Schalm, Energy flow in quantum critical systems far from equilibrium, Nat. Phys. **11**, 509 (2015).

[12] D. Bernard and B. Doyon, A hydrodynamic approach to non-equilibrium conformal field theories, J. Stat. Mech. (2016) 033104.

[13] I. Amado and A. Yarom, Black brane steady states, J. High Energy Phys. 10 (2015) 015.

[14] I. Robinson and A. Trautman, Some spherical gravitational waves in general relativity, Proc. R. Soc. A **265**, 463 (1962).

[15] R. V. Craster and O. K. Matar, Dynamics and stability of thin liquid films, Rev. Mod. Phys. **81**, 1131 (2009).

[16] G. B. de Freitas and H. S. Reall, Algebraically special solutions in AdS/CFT, J. High Energy Phys. 06 (2014) 148.

[17] I. Bakas and K. Skenderis, Non-equilibrium dynamics and AdS4 Robinson-Trautman, J. High Energy Phys. 08 (2014) 056.

[18] B. Schmidt, Existence of solutions of the Robinson-Trautman equation and spatial infinity, Gen. Relativ. Gravit. **20**, 65 (1988).

[19] A. D. Rendall, Existence and asymptotic properties of global solutions of the Robinson-Trautman equation, Classical Quantum Gravity **5**, 1339 (1988).

[20] D. Singleton, On global existence and convergence of vacuum Robinson-Trautman solutions, Classical Quantum Gravity **7**, 1333 (1990).

[21] P. T. Chrusciel, Semi-global existence and convergence of solutions of the Robinson-Trautman (2-dimensional Calabi) equation , Commun. Math. Phys. **137**, 289 (1991).

[22] P. T. Chrusciel, On the global structure of Robinson-Trautman space-times, Proc. R. Soc. A **436**, 299 (1992).

[23] I. Bakas, K. Skenderis, and B. Withers (unpublished).

[24] S. de Haro, S. N. Solodukhin, and K. Skenderis, Holographic reconstruction of spacetime and renormalization in the AdS/CFT correspondence, Commun. Math. Phys. **217**, 595 (2001).

[25] The Cotton tensor of a three-dimensional metric γ_{ab} is defined as follows: $C^{ab}=\frac{\epsilon^{acd}}{\sqrt{-\det\gamma}}\nabla_c(R^b{}_d-\frac{1}{4}\delta^b{}_dR)$, where ϵ^{acd} is the antisymmetric symbol and R_{ab}, R are the Ricci tensor and curvature scalar of the metric γ_{ab}.

[26] H. Stephani, D. Kramer, M. MacCallum, C. Hoenselaers, and E. Herlt, *Exact Solutions of Einstein's Field Equations*, 2nd ed. (Cambridge University Press, Cambridge, England, 2003).